Acta Crystallographica Section C
Crystal Structure Communications
ISSN 0108-2701

Two polymorphs of anhydrous 4-pyridone at 100 K

Aleksandra Tyl,[a]* Maria Nowak[b] and Joachim Kusz[b]

[a]Institute of Chemistry, University of Silesia, 9 Szkolna Street, PL 40-006 Katowice, Poland, and [b]Institute of Physics, University of Silesia, 4th Uniwersytecka Street, PL 40-006 Katowice, Poland
Correspondence e-mail: aleksandra.tyl@us.edu.pl

Received 13 June 2008
Accepted 15 October 2008
Online 26 November 2008

Two polymorphs of the title compound, C_5H_5NO, (I), have been obtained from ethanol. One polymorph crystallizes in the monoclinic space group *C*2/*c* [henceforth (I)-*M*], while the other crystallizes in the orthorhombic space group *Pbca* [henceforth (I)-*O*]. In the two forms, the lattice parameters, cell volume and packing motifs are very similar. There are also two independent molecules of 4-pyridone in each asymmetric unit. The molecules are linked by N—H···O hydrogen bonds into one-dimensional zigzag chains extending along the *b* axis in the (I)-*M* polymorph and along the *a* axis in the (I)-*O* polymorph, with the graph set $C_2^2(12)$. The structures are stabilized by weak C—H···O hydrogen bonds linking adjacent chains, thus forming a ring with the graph set $R_6^5(28)$. The significance of this study lies in the analysis of the hydrogen-bond interactions occurring in these structures. Analyses of the crystal structures of the two polymorphs of 4-pyridone are helpful in elucidating the mechanism of the generation of spectroscopic effects observed in the IR spectra of these polymorphs in the frequency range of the N—H stretching vibration band.

Comment

In the literature, one can find many papers concerning the powerful biological activities of derivatives of 4-pyridone, (I). Some of these derivatives are known to have potential anti-tumor effects, *e.g.* 3-acetoxy-2-methyl-4-pyridone (Hwang *et al.*, 1980). It has also been proved that some 4-pyridone derivatives exhibit a strong antibacterial effect, for instance against *Staphylococcus aureus* (Takahata *et al.*, 2007). A series of 4-pyridone derivatives have been identified and shown to possess antimicrobial properties in the case of *Staphylococcus aureus*, a group of bacteria that is resistant to triclosan. Other investigators have shown that diaryl ether-substituted 4-pyridones inhibit mitochondrial electron transport in *Plasmodium falciparum* and *Plasmodium yoelii*, meaning that they have a potential antimalarial effect (Yeates *et al.*, 2008). In the past few years, 4-pyridone has also been used as a bifunctional ligand that is capable of binding to metal centres, *e.g.* cobalt (Gao *et al.*, 2004), lanthanum (Deng *et al.*, 2005) or cadmium (Englert & Schiffers, 2006).

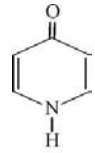

(I)

The above-mentioned compounds were investigated not only in terms of their chemical activity but also to determine their crystal structures. In the Cambridge Structural Database (CSD; Version 5.29; Allen, 2002) there are 57 records concerning derivatives of 4-pyridone, including 17 for organometallic compounds. Surprisingly, many structures of 4-pyridone derivatives have been described, but the simple compound was only known to exist in the keto form as 4-pyridone (Smith, 1979).

Jones (2001) obtained colourless crystals of 4-pyridone 1.2-hydrate by evaporating anhydrous 4-pyridone from dried acetone. He concluded that the hydrate is formed by the influence of adventitious water.

Our interest in defining the crystal structure of anhydrous 4-pyridone was the result of investigations of the IR spectra of hydrogen bonding in various compounds, such as pyridine-4-thione (Flakus *et al.*, 2002), imidazole (Flakus & Michta, 2004) and pyridine-2-thione (Flakus & Tyl, 2008). Hence, the study of the IR spectra of 4-pyridone was a natural continuation of this work. The IR spectra of 4-pyridone were measured in KBr pellets and in single crystals. The spectra showed that the compound was totally anhydrous. Moreover, the spectra showed the existence of two anhydrous forms of 4-pyridone, *viz.* a monoclinic form, (I)-*M*, and an orthorhombic form, (I)-*O*. To allow the correct interpretation of the temperature, isotopic substitution of deuterium and linear dichroism effects in IR crystalline spectra of the described compound, we have determined the crystal structures of these two polymorphs.

In the asymmetric units of (I)-*M* and (I)-*O*, there are two geometrically similar independent molecules (Figs. 1 and 2). The interplanar angles between molecules *A* and *B* are 47.71 (6) and 47.82 (3)° in forms (I)-*M* and (I)-*O*, respectively. The molecules are linked by N—H···O hydrogen bonds in the sequence *A*...*B*...*A*...*B*.... The bond lengths and angles in the 4-pyridone rings of the two polymorphs are similar and correspond well to the molecular dimensions of the pyridine rings in the hydrated form, in the sulfur analogue (Flakus *et al.*, 2002; Muthu & Vittal, 2004) and in the 4-pyridone derivatives reported in the CSD.

The only significant differences between all the independent molecules in the two structures are in the torsion angles. The 4-pyridone rings are approximately planar, but the N—H bonds lie out of the plane of the pyridone rings (Tables 1 and 3). This fact is consistent with the presence of π-electron delocalization extending from the N atom through the π system of the ring to the carbonyl group. The keto–enol

 doi:10.1107/S0108270108033660

tautomerism of 4-pyridone derivatives can be easily monitored by consideration of the geometry. In the hydroxy tautomer, the C=O bond distance is about 1.35 Å, the endocyclic angle at the N atom is significantly lower than 120°, the pyridone ring is planar and the form is more stable than the keto form (Kettmann *et al.*, 2001).

The lattice parameters and volumes of the (I)-*M* and (I)-*O* phases are surprisingly similar, with *abc* in (I)-*M* corresponding to *cab* in the (I)-*O* form. The cell volume of (I)-*M* is only about 10 Å^3 larger than that of (I)-*O* at 100 K. The real difference between these two phases is connected with their symmetry. Views of the crystal packing (Figs. 3 and 4) show the similarities and differences in the packing arrangements of the molecules, which result in the symmetries characteristic of the observed space groups.

The intermolecular hydrogen bonds observed in (I)-*O* and (I)-*M* form $C_2^2(12)$ graph-set chains (Etter *et al.*, 1990; Bernstein *et al.*, 1995) with second-level patterns *via* the path O1—C3—C2—C1—N1—H1N···O2—C8—C7—C6—N2—H2N···O1^{i}, involving two symmetry-independent N—H···O hydrogen bonds. This chain runs along the [010] direction [symmetry code: (i) $x, y+1, z$] in (I)-*M* (Fig. 5) and along the [100] direction [symmetry code: (i) $x+1, y, z$] in (I)-*O* (Fig. 6). Additionally, in both forms, atom C6 of the heterocyclic ring of molecule *B* acts as a donor in a weak intermolecular hydrogen bond with atom O2 of molecule *B* from an adjacent chain. This interaction links the molecules into a C—H···O hydrogen-bonded chain *via* glide planes along the *c*- and *b*-axis directions in (I)-*M* and (I)-*O*, respectively. The graph-set motif of *C*(5) is formed by the following path: O2—C8—C7—C6—H6···O2^{ii} (see Tables 2 and 4 for geometric parameters and symmetry codes). The infinite C—H···O-bonded chain has only one type of hydrogen bond.

The chains of N—H···O hydrogen-bonded molecules in the hydrated form of 4-pyridone (Jones, 2001) also show a tendency towards weak interaction. In contrast to the anhydrous forms, hydrated 4-pyridone displays several C—H···O interactions linking pyridone and water molecules, but no such bonds appear between the pyridone molecules.

The packing motifs are common to the two forms of 4-pyridone described here. All graph sets characterizing hydrogen bonds are presented in Table 5. There are four types of noncyclic dimer, two with the motifs for the first-level and two with the motifs for the second-level patterns. There are also two infinite chains, described above, and one $R_6^5(28)$ ring containing three different types of hydrogen bond (Figs. 5 and 6). The assignment of graph-set descriptors was performed using *RPluto* as described by Motherwell *et al.* (1999).

Although there are seven different graph-set motifs, only one of them is important for the interpretation of the IR

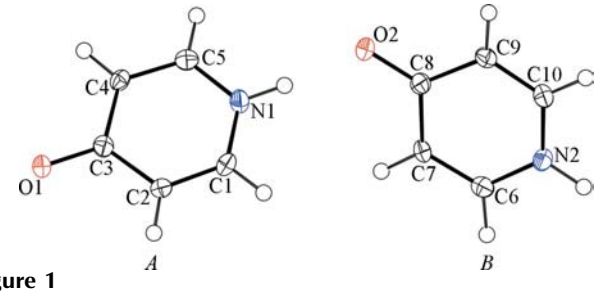

Figure 1
A view of the two independent molecules of (I)-*M*, showing the atom and molecule numbering schemes. Displacement ellipsoids are drawn at the 50% probability level.

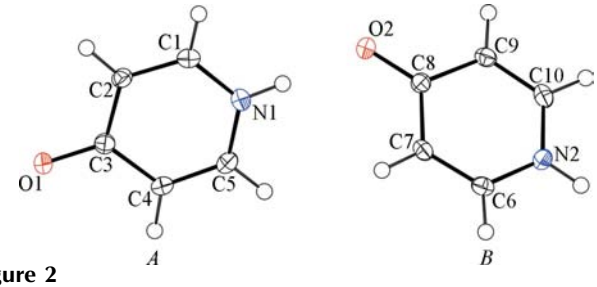

Figure 2
A view of the two independent molecules of (I)-*O*, showing the atom and molecule numbering schemes. Displacement ellipsoids are drawn at the 50% probability level.

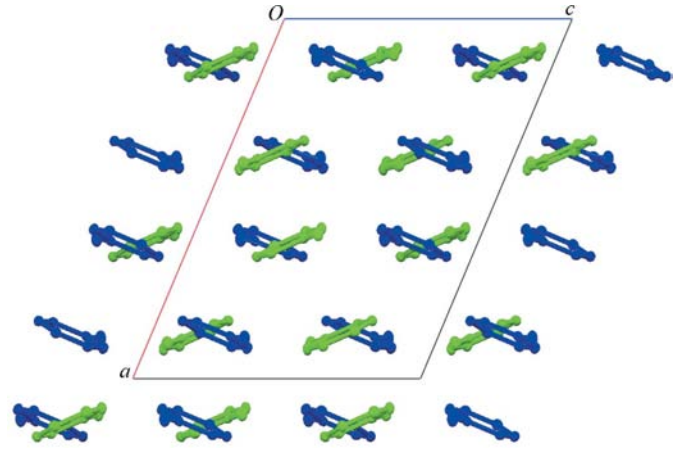

Figure 3
The packing of (I)-*M* viewed along the *b* axis. Molecules have been coloured by symmetry equivalence.

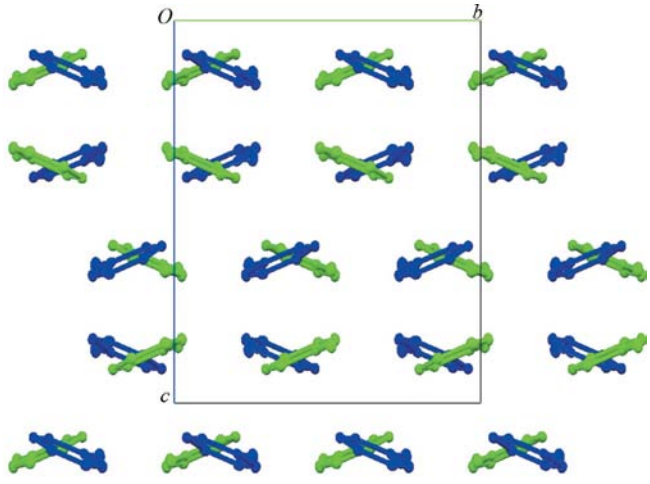

Figure 4
The packing of (I)-*O* viewed along the *a* axis. Molecules have been coloured by symmetry equivalence.

spectra. In hydrogen-bond spectroscopy, the way in which hydrogen-bonded molecules aggregate plays an important role. In the case of monoclinic and orthorhombic 4-pyridone, the crucial information received from the graph-set analysis is that the molecules are linked by N—H···O hydrogen bonds, forming an infinite chain along the *b* axis and along the *a* axis, respectively. The predominance of the N—H···O over the C—H···O hydrogen bonds follows from their energy. All the geometric parameters of the N—H···O interactions observed in both forms of the anhydrous 4-pyridone (Tables 2 and 4) are within the limits for strong hydrogen bonds defined by Desiraju & Steiner (1999). Judging from the bond distances, the N—H···O hydrogen bonds between two 4-pyridone molecules in the (I)-*M* and (I)-*O* polymorphs appear to be slightly stronger than those in hydrated 4-pyridone. In the latter compound, there are four different N—H···O hydrogen bonds excluding those between 4-pyridone and water molecules. The difference between the averages of the N···O bond distances in the hydrated and anhydrous 4-pyridone is significant at the 3σ confidence limit, while the difference between the N—H···O angles in both forms of 4-pyridone is not significant. The average of these angles in hydrated 4-pyridone is 165°.

Along with similarities in packing motifs between the monoclinic and orthorhombic 4-pyridone polymorphs there is one difference. The N—H···O hydrogen-bonded chains running in the same direction are closer in the monoclinic polymorph than in the orthorhombic polymorph. The distance between the centres of the hydrogen bonds from the adjacent chains is *ca* 3.56 Å in (I)-*M* and *ca* 3.69 Å in (I)-*O*. The shortest contact between the centres of the hydrogen bonds from two adjacent chains running in opposite directions is *ca* 4 Å in both polymorphs. This increase of the distance between the neighbouring hydrogen bonds in orthorhombic 4-pyridone is probably the cause of the observed differences between the IR spectra of the two polymorphs.

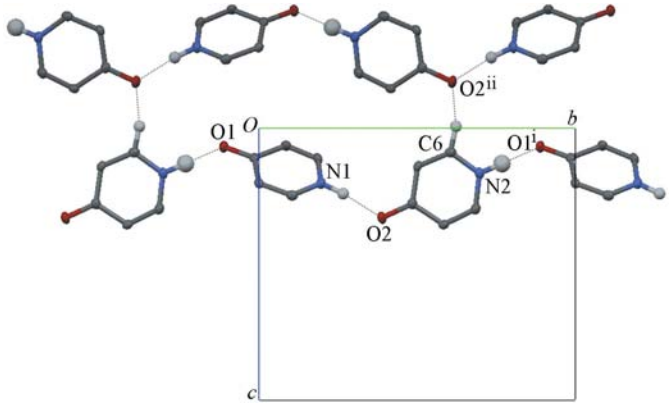

Figure 5
Part of the crystal structure of (I)-*M*, viewed along the *a* axis, showing the $C_2^2(12)$ chains and the $R_6^5(28)$ ring formed *via* three types of hydrogen bonds. [Symmetry codes: (i) $x, y+1, z$; (ii) $x, -y+1, z-\frac{1}{2}$.]

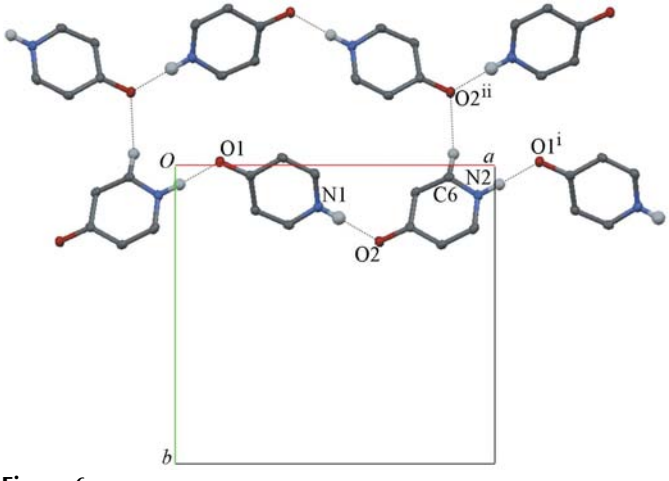

Figure 6
Part of the crystal structure of (I)-*O*, viewed along the *c* axis, showing the $C_2^2(12)$ chains and the $R_6^5(28)$ ring formed *via* three types of hydrogen bonds. [Symmetry codes: (i) $x+1, y, z$; (ii) $-x+\frac{3}{2}, y-\frac{1}{2}, z$.]

Experimental

Single crystals for X-ray analysis were obtained by dissolving anhydrous 4-pyridone (from Sigma–Aldrich) in anhydrous ethanol. The solvent was allowed to evaporate slowly in a dry air-tight glass container over a period of three weeks at room temperature. Crystals suitable for X-ray diffraction were selected directly from the sample, where crystals from both phases appeared simultaneously.

Polymorph (I)-*M*

Crystal data

C_5H_5NO
$M_r = 95.10$
Monoclinic, $C2/c$
$a = 15.137\ (6)$ Å
$b = 11.966\ (2)$ Å
$c = 11.168\ (2)$ Å
$\beta = 112.90\ (2)^\circ$
$V = 1863.4\ (9)$ Å^3
$Z = 16$
Mo $K\alpha$ radiation
$\mu = 0.10$ mm^{-1}
$T = 100\ (2)$ K
$0.4 \times 0.27 \times 0.26$ mm

Data collection

Oxford Diffraction diffractometer with Sapphire3 CCD detector
5978 measured reflections
1633 independent reflections
1452 reflections with $I > 2\sigma(I)$
$R_{int} = 0.016$

Refinement

$R[F^2 > 2\sigma(F^2)] = 0.065$
$wR(F^2) = 0.176$
$S = 1.00$
1633 reflections
137 parameters
H atoms treated by a mixture of independent and constrained refinement
$\Delta\rho_{max} = 0.72$ e Å^{-3}
$\Delta\rho_{min} = -0.26$ e Å^{-3}

Table 1
Selected geometric parameters (Å, °) for (I)-*M*.

O1—C3	1.2745 (19)	O2—C8	1.2736 (19)
N1—C5	1.353 (2)	N2—C10	1.354 (2)
N1—C1	1.356 (2)	N2—C6	1.354 (2)
C1—C2	1.353 (2)	C6—C7	1.362 (2)
C4—C5	1.363 (2)	C9—C10	1.347 (2)
C5—N1—C1	119.81 (14)	C10—N2—C6	119.71 (14)
C4—C5—N1—H1N	−171.8 (15)	C9—C10—N2—H2N	−172.3 (19)
C2—C1—N1—H1N	172.0 (15)	C7—C6—N2—H2N	172 (2)

Table 2
Hydrogen-bond geometry (Å, °) for (I)-*M*.

D—H···*A*	*D*—H	H···*A*	*D*···*A*	*D*—H···*A*
N1—H1N···O2	0.93 (2)	1.73 (2)	2.6567 (19)	172 (2)
N2—H2N···O1^{i}	0.96 (3)	1.71 (3)	2.6575 (18)	172 (3)
C6—H6···O2^{ii}	1.003 (19)	2.506 (19)	3.258 (2)	131.6 (14)

Symmetry codes: (i) $x, y+1, z$; (ii) $x, -y+1, z-\frac{1}{2}$.

Polymorph (I)-*O*

Crystal data

C_5H_5NO
M_r = 95.10
Orthorhombic, *Pbca*
a = 11.953 (2) Å
b = 11.146 (2) Å
c = 13.914 (3) Å
V = 1853.7 (6) Å^3
Z = 16
Mo *K*α radiation
μ = 0.10 mm^{-1}
T = 100 (2) K
0.50 × 0.34 × 0.16 mm

Data collection

Oxford Diffraction diffractometer with Sapphire3 CCD detector
11099 measured reflections
1626 independent reflections
1356 reflections with $I > 2\sigma(I)$
R_{int} = 0.018

Refinement

$R[F^2 > 2\sigma(F^2)]$ = 0.037
$wR(F^2)$ = 0.111
S = 1.00
1626 reflections
137 parameters
H atoms treated by a mixture of independent and constrained refinement
Δρ$_{max}$ = 0.32 e Å^{-3}
Δρ$_{min}$ = −0.24 e Å^{-3}

Table 3
Selected geometric parameters (Å, °) for (I)-*O*.

O1—C3	1.2696 (15)	O2—C8	1.2695 (15)
N1—C1	1.3478 (16)	N2—C6	1.3501 (16)
N1—C5	1.3532 (17)	N2—C10	1.3547 (17)
C1—C2	1.3582 (17)	C6—C7	1.3568 (17)
C4—C5	1.3524 (18)	C9—C10	1.3556 (18)
C1—N1—C5	119.78 (11)	C6—N2—C10	119.76 (11)
C4—C5—N1—H1N	−170.5 (12)	C9—C10—N2—H2N	171.2 (10)
C2—C1—N1—H1N	170.9 (12)	C7—C6—N2—H2N	−171.1 (11)

Table 4
Hydrogen-bond geometry (Å, °) for (I)-*O*.

D—H···*A*	*D*—H	H···*A*	*D*···*A*	*D*—H···*A*
N1—H1N···O2	0.871 (19)	1.787 (19)	2.6526 (14)	172.0 (15)
N2—H2N···O1^{i}	0.902 (17)	1.754 (17)	2.6523 (14)	174.3 (14)
C6—H6···O2^{ii}	0.963 (14)	2.530 (14)	3.2552 (16)	132.1 (10)

Symmetry codes: (i) $x+1, y, z$; (ii) $-x+\frac{3}{2}, y-\frac{1}{2}, z$.

H atoms involved in hydrogen bonding were located in a difference Fourier map and their positional parameters were refined freely (refined bond lengths are given in Tables 2 and 4). The remaining aromatic H atoms were treated as riding on their parent C atoms (C—H = 0.95 Å). All H atoms were assigned U_{iso} values equal to 1.2U_{eq} of the parent C or N atom, except for atoms H1N, H2N and H6 in (I)-*M* and (I)-*O*, for which the U_{iso}(H) values were refined.

Table 5
Graph sets for the two anhydrous polymorphs of 4-pyridone.

First-level motifs		Higher-level motifs	
Graph notation	Hydrogen bond connecting the molecules	Graph notation	Hydrogen bonds connecting the molecules
D(2) *a*	N1—H1N···O2	$C_2^2(12)$ *>a>b*	N1—H1N···O2, N2—H2N···O1^{i}
D(2) *b*	N2—H2N···O1^{i}	$D_2^3(8)$ *a&c*	N1—H1N···O2, C6—H6···O2^{ii}
C(5) *c*	C6—H6···O2^{ii}	$D_3^3(12)$ *b&c*	N2—H2N···O1^{i}, C6—H6···O2^{ii}
		$R_6^5(28)$ *abc*	N1—H1N···O2, N2—H2N···O1^{i}, C6—H6···O2^{ii}

Symmetry codes are as given in Tables 2 and 4.

For both polymorphs, data collection: *CrysAlis CCD* (Oxford Diffraction, 2006); cell refinement: *CrysAlis RED* (Oxford Diffraction, 2006); data reduction: *CrysAlis RED*; program(s) used to solve structure: *SHELXS97* (Sheldrick, 2008); program(s) used to refine structure: *SHELXL97* (Sheldrick, 2008); molecular graphics: *PLATON* (Spek, 2003) and *Mercury* (Macrae *et al.*, 2006); software used to prepare material for publication: *publCIF* (Westrip, 2008).

Supplementary data for this paper are available from the IUCr electronic archives (Reference: AV3155). Services for accessing these data are described at the back of the journal.

References

Allen, F. H. (2002). *Acta Cryst.* B**58**, 380–388.
Bernstein, J., Davis, R. E., Shimoni, L. & Chang, N.-L. (1995). *Angew. Chem. Int. Ed. Engl.* **34**, 1555–1573.
Deng, Z.-P., Gao, S., Huo, L.-H. & Zhao, H. (2005). *Acta Cryst.* E**61**, m2523–m2525.
Desiraju, G. R. & Steiner, T. (1999). *The Weak Hydrogen Bond in Structural Chemistry and Biology*. New York: Oxford University Press.
Englert, U. & Schiffers, S. (2006). *Acta Cryst.* E**62**, m194–m195.
Etter, M. C., MacDonald, J. C. & Bernstein, J. (1990). *Acta Cryst.* B**46**, 256–262.
Flakus, H. T. & Michta, A. (2004). *J. Mol. Struct.* **707**, 17–31.
Flakus, H. T. & Tyl, A. (2008). *Vib. Spectrosc.* **47**, 129–138.
Flakus, H. T., Tyl, A. & Jones, P. G. (2002). *Spectrochim. Acta*, **58**, 299–310.
Gao, S., Lu, Z.-Z., Huo, L.-H., Zhao, H. & Zhao, J.-G. (2004). *Acta Cryst.* E**60**, m609–m610.
Hwang, D. R., Proctor, G. R. & Driscoll, J. S. (1980). *J. Pharm. Sci.* **69**, 1074–1076.
Jones, P. G. (2001). *Acta Cryst.* C**57**, 880–882.
Kettmann, V., Světlík, J. & Kratky, C. (2001). *Acta Cryst.* C**57**, 590–592.
Macrae, C. F., Edgington, P. R., McCabe, P., Pidcock, E., Shields, G. P., Taylor, R., Towler, M. & van de Streek, J. (2006). *J. Appl. Cryst.* **39**, 453–457.
Motherwell, W. D. S., Shields, G. P. & Allen, F. H. (1999). *Acta Cryst.* B**55**, 1044–1056.
Muthu, S. & Vittal, J. J. (2004). *Cryst. Growth Des.* **4**, 1181–1184.
Oxford Diffraction (2006). *CrysAlis CCD* and *CrysAlis RED*. Oxford Diffraction Ltd, Wrocław, Poland.
Sheldrick, G. M. (2008). *Acta Cryst.* A**64**, 112–122.
Smith, D. M. (1979). *Pyridines*, in *Comprehensive Organic Chemistry*, Vol. 4, edited by P. G. Sammes, pp. 3–84. Oxford: Pergamon Press.
Spek, A. L. (2003). *J. Appl. Cryst.* **36**, 7–13.
Takahata, S., Iida, M., Yoshida, T., Kumura, K., Kitagawa, H. & Hoshiko, S. (2007). *J. Antibiot.* **60**, 123–128.
Westrip, S. P. (2008). *publCIF*. In preparation.
Yeates, C. L. *et al.* (2008). *J. Med. Chem.* **51**, 2845–2852.